UNIVERSITY OF ILLINOIS

December 9, 1988

THIS IS TO CERTIFY THAT THE THESIS PREPARED UNDER MY SUPERVISION BY

Martha Ann Shaw

ENTITLED The Ubiquitous Nature of Metastable Droplets in the Ambient

Atmosphere

IS APPROVED BY ME AS FULFILLING THIS PART OF THE REQUIREMENTS FOR THE

DEGREE OF Bachelor of Science in Chemistry

Steven A Zumdahl Mark L Ward

Instructor in Charge

APPROVED: [signature]

HEAD OF DEPARTMENT OF Chemistry

O-1364

The Ubiquitous Nature of Metastable Droplets in the Ambient Atmosphere

Senior Research Thesis
Department of Chemistry

Martha Ann Shaw

December 9, 1988

Table of Contents

Introduction

The atmosphere is composed of gases, liquid droplets and solid particles in constant movement and flux. Aerosols are, generally, multicomponent particles which range in diameter from roughly 0.01 to 10 μm. They can be solid or liquid or a combination of both phases. They can be directly introduced into the atmosphere by any number of sources, or be formed in the atmosphere by coagulation, nucleation or gas-to-particle conversion.

Atmospheric aerosol particles with diameters < 2 μm consist primarily of sulfates, nitrates and ammonium in the form of inorganic salts such as $(NH_4)_2SO_4$, HNO_3 NH_4NO_3, and Na_2SO_4 (1,2,3). These compounds are all hygroscopic and as such will exhibit properties that are dependent on the amount of H_2O available in the atmosphere, measured by the relative humidity (RH), such as size, phase, liquid H_2O content and thermodynamic state. The interaction of these salts with liquid H_2O in the ambient atmosphere has been the topic of much atmospheric research.

Liquid H_2O is common in the atmosphere and plays a major role in the chemistry, physics and general thermodynamics of the atmosphere. The conversion of SO_2 to particulate sulfate occurs partially in liquid H_2O droplets and its rate is dependent on the amount of available H_2O (4,5). The equilibrium products, vapor pressures and dissociation constants of many atmospheric compounds are functions of the RH such as for the system of HNO_3, NH_4NO_3, NH_3 and H_2O (6,7).

The impact of RH on light scattering and thus on visibility degradation is still a topic of much debate (8,9). The primary impact of humidity on visibility is known to be its effect on particle size. Ambient aerosols, especially hygroscopic particles, will increase in size with increasing RH, which will change their light scattering characteristics (9).

Rates of surface-limited mass transfer reactions will increase with RH due to the increased surface area. Particle aerodynamics will be impacted by RH as the size of a particle greatly effects its rate of travel, falling and coagulation.

The interaction of liquid H_2O with hygroscopic, deliquescent inorganic salts is of primary interest. Aqueous droplets containing these compounds will have all of the characteristics mentioned above, with some additional unique properties. The following section will explain the behavior of these salts with liquid H_2O in the ambient atmosphere, how these droplets become metastable, and why they are of interest.

Deliquescent Aerosols

A hygroscopic aerosol will respond to changes in relative humidity in one of the following ways (Fig. 1)[Reprinted with Permission: Rood, M.J., et. al., Tellus, 39B, 385-397 (1987)](11). A non-deliquescent hygroscopic aerosol will show a direct correlation between its size and RH (Fig. 1A). The attached H_2O will be constantly saturated in solute until the solute is completely dissolved. A droplet containing a single deliquescent salt displays an abrupt phase change with both increasing and decreasing RH. This droplet at sufficiently low RH (Fig 1B, Curve a) will be in its dry crystalline state. As RH increases along Curve a, H_2O adsorbs onto the particle, but none of the compound dissolves into the adsorbed H_2O. At some RH value which is the deliquescence humidity, the compound abruptly dissolves into solution to form a droplet saturated with solute ions (Fig. 1B, Curve b). At increasing RH values, the amount of H_2O increases, and the droplet becomes subsaturated (Fig 1B, Curve c). Upon decreasing RH, the solute does not recrystallize at the deliquescence humidity but remains as a droplet which is supersaturated with respect to solute concentration (Fig 1B, Curve d). This region represents the metastable droplet. It occurs because the supersaturated solution is at a local minimum in Gibbs free energy. This persists until the supersaturation is so great (RH is so low) as to force nucleation. At this RH efflorescence occurs (Fig 1B, Curve e), the solute crystallizes and the attached liquid H_2O is driven off leaving only the dry crystalline particle. This droplet exhibits hysteresis, because its properties are path dependent. A droplet containing two deliquescent salts can display multiple phase changes (Fig 1C). The first deliquescence (Fig 1C, Curve a) is one of the species in the dry core entering the solution abruptly. The second deliquescence Fig 1C, Curve b) is due to the second compound dissolving, resulting in a saturated, homogeneous liquid droplet.

A droplet may contain a mixture of deliquescent compounds and insoluble material. The insoluble material will provide a nucleation center, thus allowing nucleation at a much lower level of supersaturation. In this case, a metastable droplet may form for either a small range, or not at all.

As will be shown, metastable droplets do occur in the ambient atmosphere. Recognition of their occurrence is important for a number of reasons. Metastable droplets occur at a lower RH than liquid H_2O droplets of the same size. They are larger than one would expect from a non-deliquescent aerosol which would be in its crystalline state at the RHs at which metastability occurs. Both of these characteristics mean that metastable droplets scatter more light than their dry counterparts. Metastable droplets also occur for longer time periods than liquid droplets under decreasing RH conditions. Thus liquid H_2O, important for all of the reasons described above, is present in the atmosphere under unfavorable conditions.

Deliquescence humidities for compounds commonly found in the ambient atmosphere are presented in Table 1 (12).

Figure 1

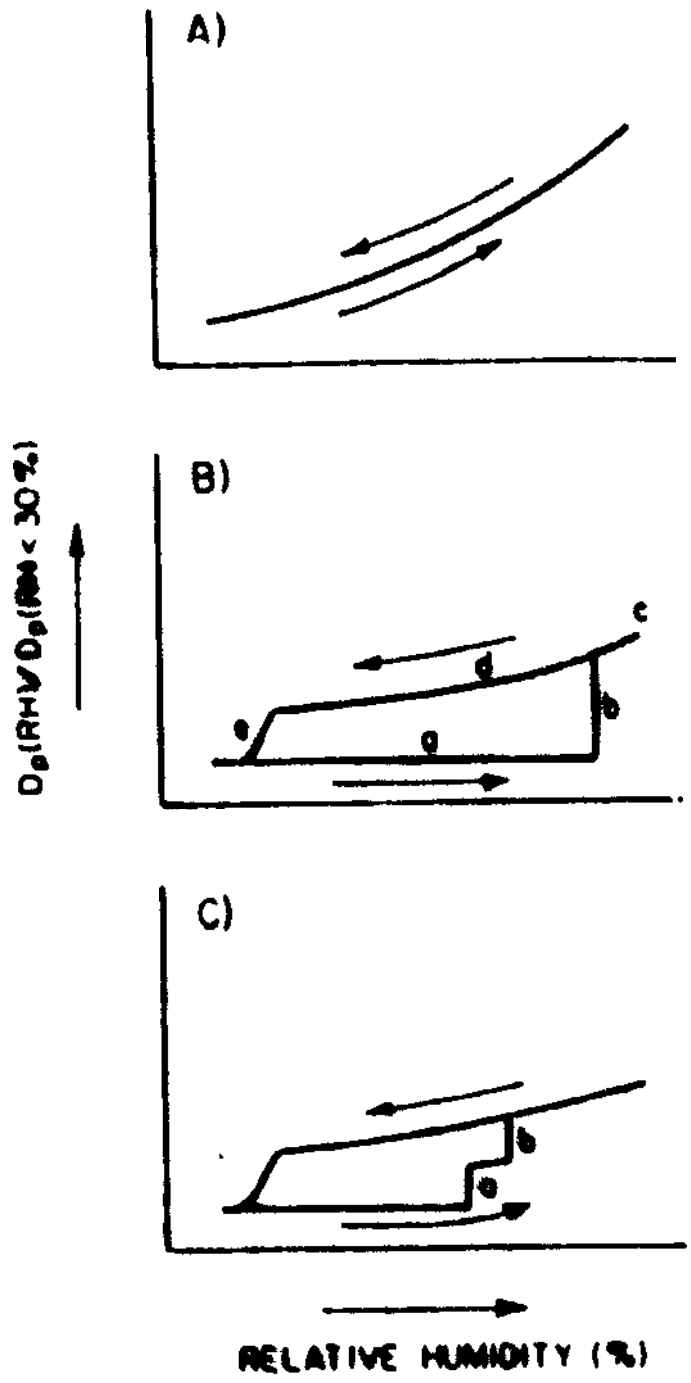

Table 1

Deliquescence Humidities for Inorganic Compounds Common to the Ambient Atmosphere

Pilinis, C. & Seinfeld, J.H. Atmospheric Environment, 21, 2453-2466 (1987).

Species	Deliquescence Humidity
$NaCl$	76.0
Na_2SO_4	93.0
$NaNO_3$	74.0
NH_4Cl	80.0
$(NH_4)_2SO_4$	80.0
NH_4HSO_4	40.0
NH_4NO_3	62.0
$NaHSO_4$	52.0
$(NH_4)_3H(SO_4)_2$	69.0

Assuming a dry crystalline salt experiencing increasing relative humidities, the salt will not dissolve until the relative ambient humidity reaches the deliquescence humidity. For humidities above a given deliquescence value, none of the solid component may exist. At humidities below these values the solid may or may not exist, dependent on thermodynamic conditions. For example, a dry particle of pure $(NH_4)_2SO_4$ would adsorb water, but not dissolve until the relative humidity reached 80%. At 80% an abrupt change in the light scattering properties of the droplet would occur.

Metastable solutions are extremely difficult to study under laboratory conditions. There cannot be a readily available nucleation site for the supersaturated solute to condense around, or the metastable state will not be reached. Bulk solution experimentation will not show a metastable state of the solute. Not until recently have metastable droplets been seen experimentally (12-15).The general occurrence of metastable droplets in the ambient atmosphere has been discovered in this project. The frequency of their occurrence is reported and their impact on ambient light scattering.

Theoretical

The metastable state exists at a local minimum of Gibb's free energy. A non-deliquescent compound (i.e. Fig. 1a) would not display metastability. The Gibb's free energy of the compound would decrease directly upon decreasing RH conditions. The solute would crystallize continuously as the amount of available H_2O was decreased, and the concentration of the solute dissolved in the H_2O would remain constant. A deliquescent particle is described by a more complicated path. Instead of decreasing directly with increasing solute saturation, the free energy of the particle decreases, then increases until it reaches a secondary maximum at a given supersaturation. This is the energy barrier to efflorescence which allows metastable droplets to form. Energy must be added in one form or another to induce nucleation in the metastable droplet.

Until 1976, theoretical calculations of multicomponent aqueous solutions present in the atmosphere were all but non-existent. Only within the last decade has there been a real attempt to calculate the activities of the components in these solutions and to understand and model their phase behavior (17,18,19,20).

The growth of saturated solution droplets at constant temperature and pressure can be followed theoretically with (17):

$$\ln \frac{p}{p^o} = \ln \gamma_1 X_1 + \frac{2 v_1 \sigma}{R T r_e}$$

The equilibrium size, r_e, of a droplet is related to the H_2O activity, $a_1 = \frac{p}{p^o}$ which for a saturated solution also equals the relative ambient humidity. γ_1 is the activity coefficient of the solution, X_1 is the mole fraction of H_2O present, σ is the surface tension of the droplet, v_1 is the partial molar volume of H_2O, p is the constant pressure assumed, p^o is the partial vapor pressure of H_2O, T is the temperature and R is the gas-law constant. This equation is valid for any multicomponent system and requires knowledge only of the solution properties. However, curvature effects can be ignored for particles of diameter > 0.1 μm (17). For these droplets the equation simplifies to: $\frac{p}{p^o} = \gamma_1 X_1$: which at high dilutions is Raoult's law.

Development of this general equation allows us to calculate relative humidity, activity coefficient or mole fraction assuming we know the other two variables. The apparent simplicity of the equation is unfortunately deceptive. Many variables must be known for the calculation of the H_2O activity and the activity coefficient. Well developed models have been proposed for calculating these variables for multicomponent solutions, which have been compared for their validity and limitations(20).

Solution activities in both the $(NH_4)_2SO_4/NH_4SO_3/H_2O$ system (21) and the $(NH_4)_2SO_4/Na_2SO_4/H_2O$ system (22) have been measured. The complexity of the many phases of these systems is best presented in phase diagrams, so both systems are presented in such a manner. Before discussion of these, a brief summary of the interpretation of phase diagrams is in order.

Phase Diagrams

Consider a general representation of a system of two salts, A and B. as solutes and H_2O (Fig 2). At any origin, i.e. point A, there is 100% of that component present. Along any axis connecting two pure species, the third species is completely absent and the concentrations of the two species are determined by the respective line segment lengths. For example, the solution at point c is composed entirely of H_2O and B, with a B to H_2O ratio given by $\frac{length\ of\ line\ B-c}{length\ of\ line\ H_2O-c}$. Point a is the solubility of pure A in solution, point b, the solubility of pure B. The solubility of each is reduced as the two are mixed. This is commonly the case, but not necessarily true for all salt solutions. The lowest solubility possible at this constant temperature is seen a point E.

Any line drawn from one origin to the opposite axis contains a constant ratio of the axis components. For example, the line through g and h has a constant A/B ratio with varying H_2O content. A typical dry ambient aerosol may follow the g-h line as it accumulates H_2O. It starts as a dry particle with ratio A/B given by Ad/Bd. As a small amount of H_2O adsorbs onto the particle, its composition is described by a point increasing up the tie line to e. Here the droplet looks like a saturated liquid with saturation composition given by E and some solid A and B. As more H_2O adsorbs, the particle reaches point g. At g all solid B dissolves. The H_2O activity is still given by E. As previously mentioned, H_2O activity is equal to relative humidity for saturated solutions, so E can be thought of to be the first dissolution point, or first deliquescence point of the mixture. As yet more H_2O is added to the droplet, it goes through the region containing liquid with dissolved B, some dissolved A, and some solid A. Throughout this region A is continuously dissovling, but no more B, as it is already completely dissolved. It follows therefore, that the mass of dissolved A increases with respect to B. The H_2O activity approaches h as more A dissolves. At point h, all of component A dissolves and the H_2O activity is given by the concentrations at h. This point can be thought of as the second deliquescence humidity (H_2O activity) for the compound. As still more H_2O condenses onto the droplet, the solution becomes more dilute.

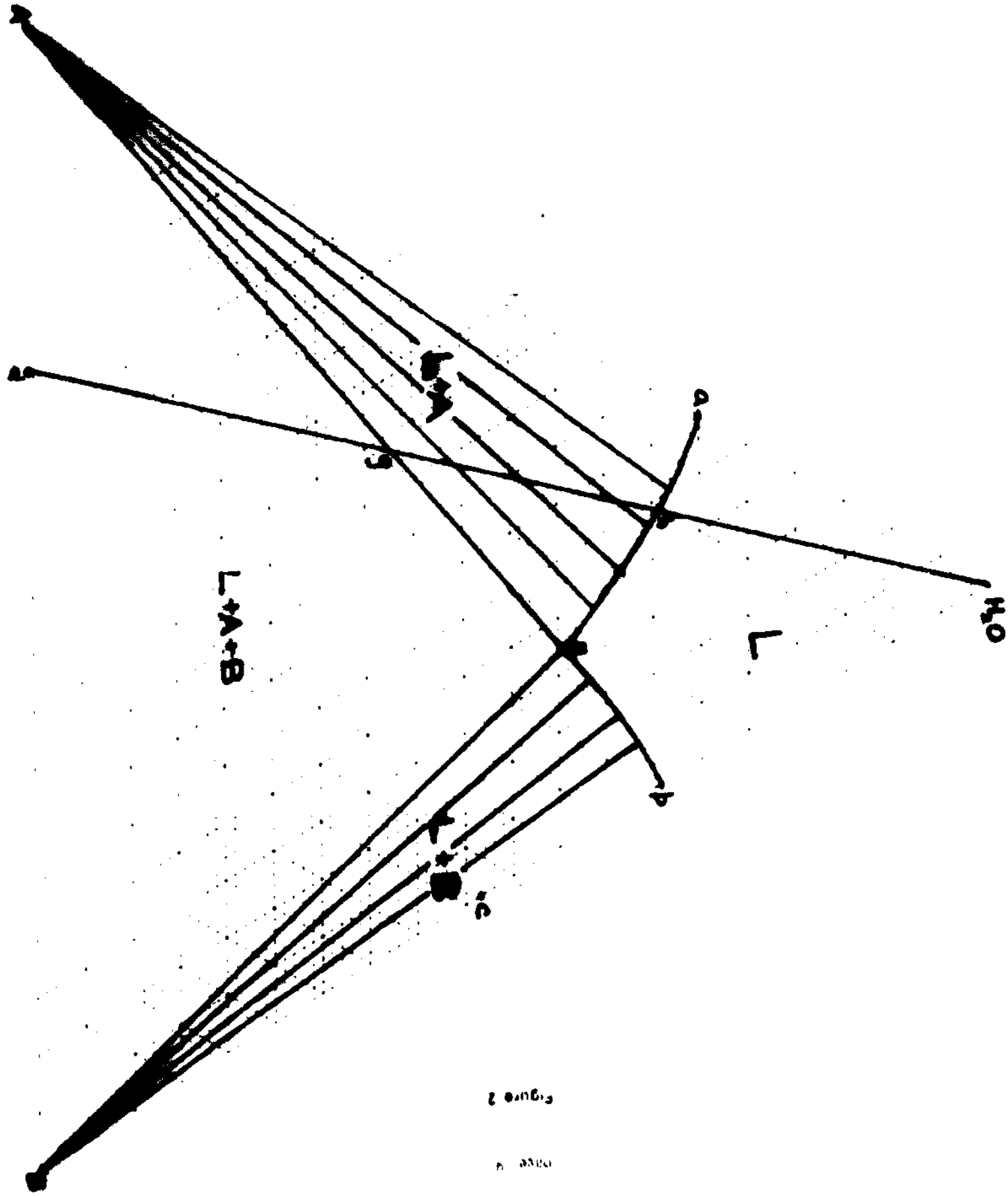

Figure 2

The previous discussion of phase diagrams assumes that there are no impediments to any phase changes. In reality, phase changes can cover an entire spectrum of time scales depending on the energy barrier to the change. Thus, the deliquescent particles will behave exactly as the binary salt mixtures presented here with two differences in interpretation.

Generally, one may assume that upon addition of H_2O to the initial dry solid, the solution is saturated with one or another of the components until they are both totally dissolved. However, a deliquescent particle will not follow this interpretation. Throughout the region between d and g (Graph 2), H_2O will adsorb onto the dry particle, but none of the salt will dissolve into solution. At point g, component B will deliquesce and the solution will be momentarily saturated with B. None of component A will dissolve until point h. Thus, the droplet can be thought of as two non-interacting phases, liquid and solid, until the first deliquescence point. The H_2O activity between d and g cannot be described by point E, but rather the H_2O retains an activity of 1 until point g. At g the H_2O activity suddenly changes to E as all of B dissolves. This H_2O activity increases from g to h with dilution of the H_2O-B solution. At point h all of component A dissolves and the H_2O activity is described by h. Upon addition of yet more H_2O, the solution becomes more dilute and the H_2O activity increases towards unity.

The other limitation to interpreting general phase diagrams for atmospheric salts is their failure to display the regions of metastability. These phase diagrams would have one believe that the solutions follow the same path as for condensation and evaporation of H_2O. Since phase diagrams are normally made from data taken under laboratory conditions (bulk solutions), this omission is understandable. This is not true in the atmosphere, however. Phase diagrams which include metastable regions have been constructed for other compounds (23). The phases of the solution upon addition of one component, i.e. H_2O, are shown with solid lines, the response upon removal of the component are shown with dashed lines. Such regions have not yet been added to diagrams of mixtures in the atmosphere, but when enough data is compiled, such regions will aid in the understanding of metastable droplets. As the phase diagrams are presently drawn, they are applicable only for increasing liquid H_2O content. In this direction along any constant mixture ratio line the possibility of the creation of metastable solutions is not a concern. Upon diminishing H_2O content at RH < the maximum deliquescence humidity, the curves signifying phase changes will be located at lower H_2O concentration than presently indicated.

The two phase diagrams of specific interest are for mixtures of $NH_4NO_3/(NH_4)_2SO_4/H_2O$ and $Na_2SO_4/(NH_4)_2SO_4/H_2O$ (Fig 3 & 4). The one unique aspect to these is the multiple regions showing the different solids formed. The $NH_4NO_3/(NH_4)_2SO_4/H_2O$ system (Graph 3) has four regions in which different solids will be seen. Region I depicts the solutions for which pure solid NH_4NO_3 will be seen. Mixtures in regions II and III and IV will contain solid $3NH_4NO_3(NH_4)_2SO_4$, $2NH_4NO_3(NH_4)_2SO_4$ and $(NH_4)_2SO_4$,respectively. The regions described by two numerals, i.e. I & II, will contain mixtures of the two components. Thus, region IV will contain solid $(NH_4)_2SO_4$ in a solution of dissolved $2NH_4NO_3(NH_4)_2SO_4$ and H_2O. Region III is more complex. For example, a solid can originally be of composition described by point j. As H_2O is added, the solid NH_4NO_3 dissolves. The mixture is then solid $3NH_4NO_3(NH_4)_2SO_4$ in a solution of NH_4NO_3 and H_2O. Upon the addition of more H_2O, H_2O dissociates some of the NH_4NO_3 in the solid compound. Thus a new compound is created, $2NH_4NO_3(NH_4)_2SO_4$. The region II & III contains these two solid compounds with the dissolved NH_4NO_3. As the equilibrium $3NH_4NO_3(NH_4)_2SO_4 \dashrightarrow 2NH_4NO_3(NH_4)_2SO_4 + NH_4NO_3$ is driven to the right upon the addition of more water, the solution enters region III. The other regions are explained in the same manner.

The diagram of the $Na_2SO_4/(NH_4)_2SO_4/H_2O$ system includes hydration formation as well as salts. Region I solutions will contain solid $Na_2SO_4\ 10H_2O$. Mixtures in region II will contain pure solid Na_2SO_4 . Regions III and IV will contain $Na(NH_4)SO_4\ 2H_2O$ and solid $(NH_4)_2SO_4$, respectively.

The deliquescence humidities of ambient aerosols are temperature dependent (18). Two-dimension phase diagrams, such as these, depict the phase changes of the mixture at constant temperature and pressure. It is possible to construct prismatic phase diagrams which show the impact of temperature or pressure on the phase changes. The approximation of constant temperature and pressure will be assumed.

Phase diagrams cannot be used for decreasing humidity conditions because while this interpretation of the diagram assumes that there is no impediment to crystallization, such an impediment does exist. A saturated droplet will not effloresce until the solution is supersaturated enough to initiate nucleation.A discussion of nucleation processes is invaluable to understanding this behavior.

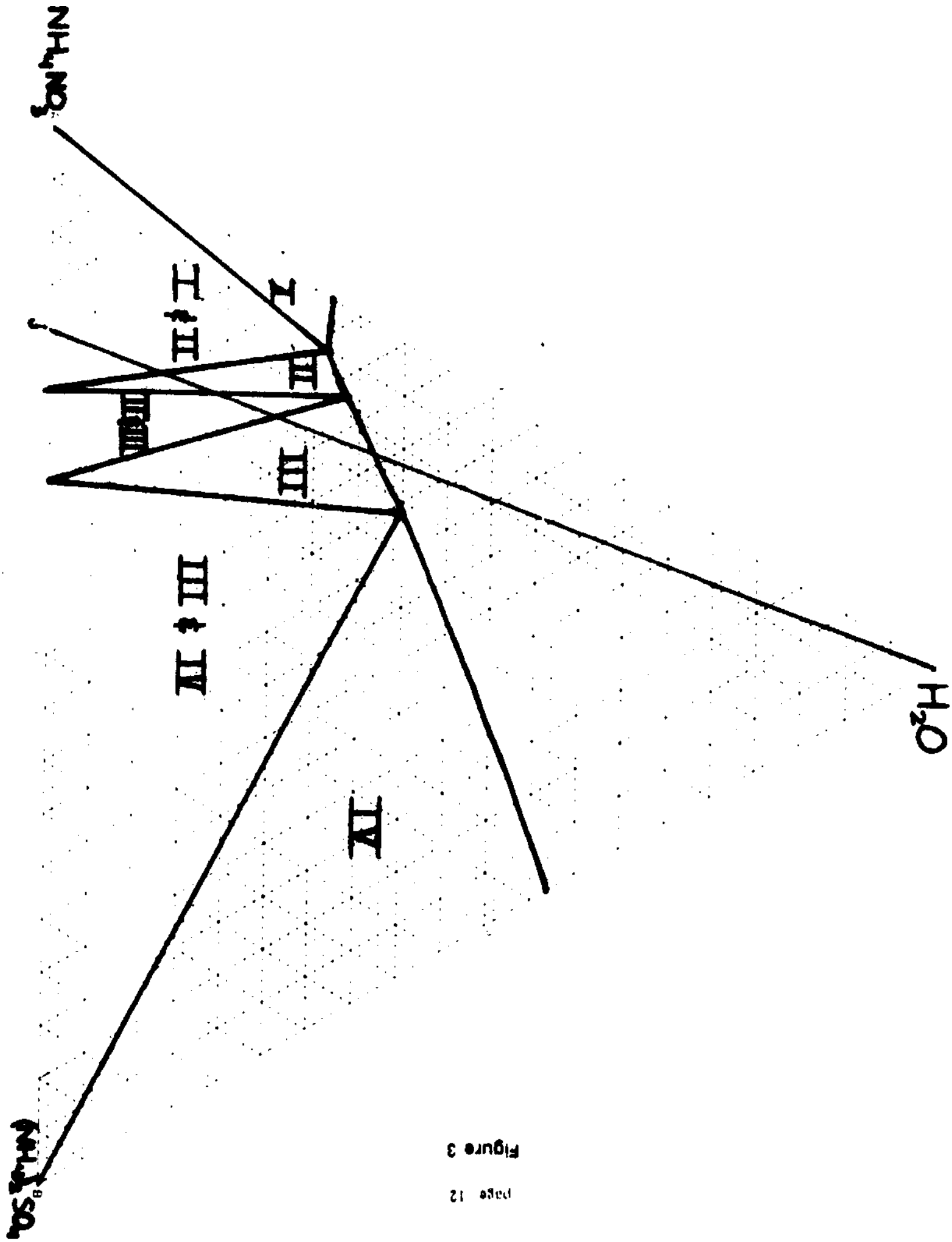

Figure 3

Figure 4

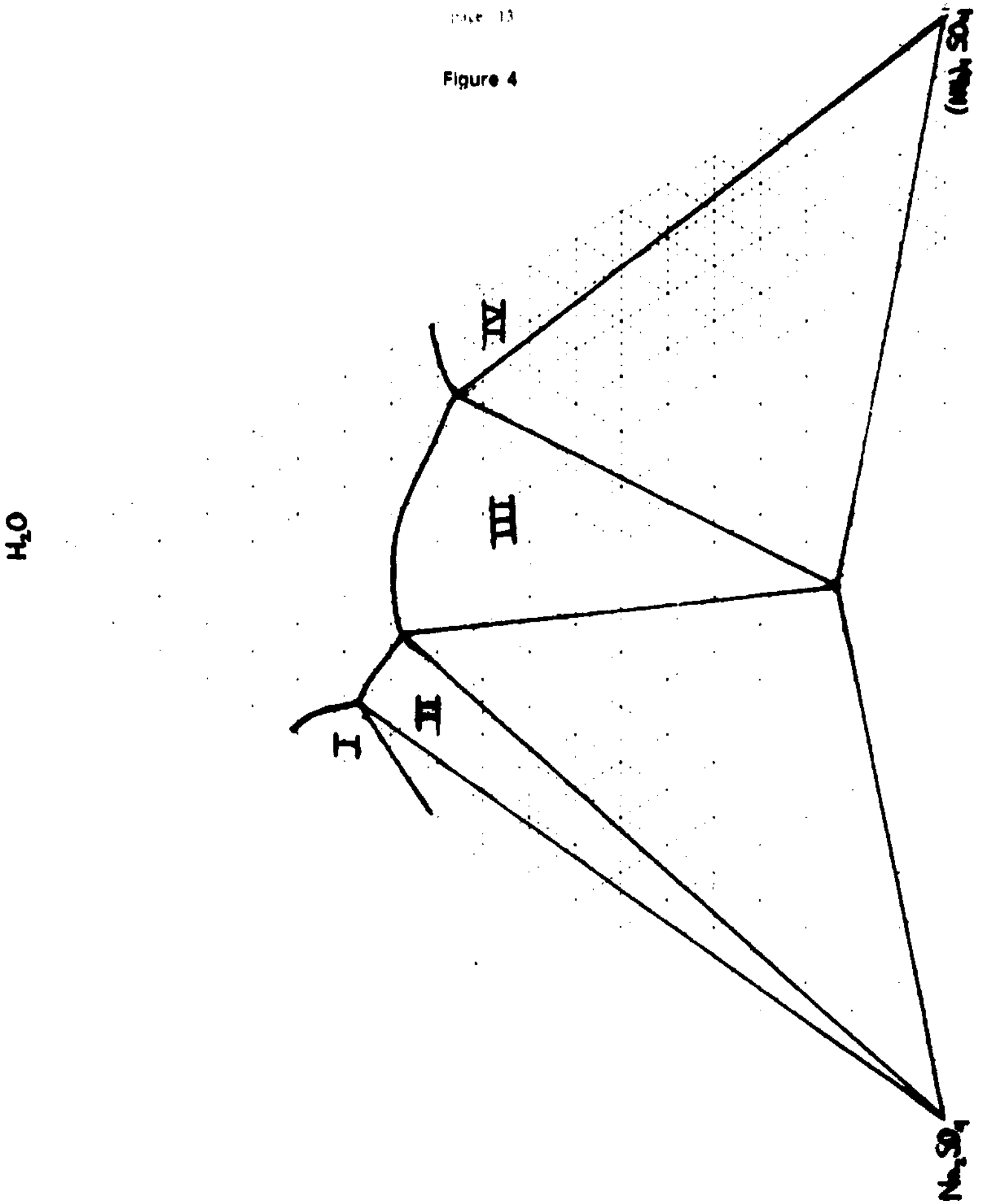

Nucleation Theory

The height of the energy barrier between metastability and efflorescence determines the stability of the metastable state. The energy barrier will normally be overcome by atmospheric particles by one of the following mechanisms: 1) supersaturation of the solution by a sufficient decrease in relative humidity which increases the internal energy of the droplet and causes homogeneous nucleation; 2) supersaturation of the droplet around an insoluble material, known as heterogeneous nucleation; 3) impaction of the droplet on a surface or with another aerosol.

All three of these mechanisms occur in the ambient atmosphere. They are all important in the destabilization of the metastable state resulting in efflorescence. Impaction is beyond the scope of nucleation theory. Homogeneous and heterogeneous nucleation will both be discussed briefly, however.

Of primary interest in the first case is homogeneous, heteromolecular nucleation. This occurs in droplets which do not contain insoluble nucleating sites, but are composed of a mixture of soluble compounds. In atmospheric conditions heteromolecular nucleation with H_2O occurs many orders of magnitude faster than homogeneous, homomolecular nucleation because the former may take place when a solution mixture is subsaturated with respect to any of the pure components as long as it is saturated with respect to the critical solution (24).

The driving force for binary homogeneous nucleation is the geometric mean saturation as presented in equation 1 (25).

$$S = S_1^{X1} S_2^{X2} \qquad Eq.1$$

where S_1 , S_2 , ... are the saturation ratios of gaseous components 1,2,... and the mole fractions of the components are X_1 , X_2 ,.... Scott and Cattrell (26) calculated for $(NH_4)_2SO_4$ as shown in equation 2.

$$S_{(NH_4)_2SO_4} = S_{NH_3}^{2/3} S_{H_2SO_4}^{1/3} \qquad Eq.2$$

where the saturation ratio of a gaseous component is the ratio of the ambient pressure to the equilibrium partial pressure of the component. In the same manner, the geometric mean saturation for NH_4NO_3 is given by equation 3.

$$S_{NH_4NO_3} = S_{NH_3}^{1/2} S_{HNO_3}^{1/2} \qquad Eq.3$$

where $S_{NH_3} = \dfrac{P_{NH_3}(amb)}{P_{NH_3}(eq)}$ and $S_{HNO_3} = \dfrac{P_{HNO_3}(amb)}{P_{HNO_3}(eq)}$ $\qquad Eq.4$

In this manner one can calculate the mean saturation and thus the nucleation rate for a given solution. Although only binary solutions (H_2O and one salt) are considered with this method, it can be expanded to multicomponent solutions. However, even with this simple example, with the saturation products as driving forces for nucleation it is evident why homogeneous nucleation occurs in the ambient atmosphere for both species.

Another way to think of homogeneous nucleation is by considering the height of the free energy barrier between the supersaturated solution and the nucleating droplet. The height of the free energy barrier to nucleation, ΔG, is dependent on the radius r of the nucleating cluster of atoms or molecules for a given supersaturation ratio. A cluster must exceed r^*, the critical nucleus radius corresponding to the maximum possible energy change, ΔG^*. Only when a cluster radius exceeds r^* will the spontaneous efflorescence follow (27).

The free energy difference of the supersaturated droplet to the dry crystalline particle is given by equation 5.

$$\Delta G_v = G^L - G^S \qquad Eq.5$$

which is the difference of the free energy of the solute per unit volume in the solid phase (G^S) to that of the liquid phase (G^L) (28). This can be related to the chemical potentials of each phase by equation 6 (17).

$$\Delta G_v = (\mu^L - \mu^S)\frac{\varrho}{MW} \qquad Eq.6$$

where μ^S is the chemical potential of the solute in a nucleus of size r and μ^L is the chemical potential of the solute in the saturated solution. ϱ is the crystalline nucleus density and MW is the molecular weight of the solute. The critical radius can be related to the maximum free energy barrier by equation 7 (29).

$$r^* = \frac{2\gamma}{\Delta G_v} \qquad Eq.7$$

where γ is the free energy of the solid/liquid interface. Thus the resulting free energy change is described by equation 8.

$$\Delta G^* = \frac{16\pi\gamma^3}{3(\Delta G_v)^2} = \frac{16\pi\gamma^3 MW^2}{3(m\mu^L - \mu^S)^2\varrho^2} \qquad Eq.8$$

Nucleation which occurs on preexisting particles is heterogeneous nucleation. As in homogeneous nucleation, the droplets must reach a critical value of supersaturation before the droplet will crystallize. The greater the droplet's supersaturation, the smaller the critical radius.

Heterogeneous nucleation is dependent on the 'wetting' angle Θ, which is a property of the nucleus shape, usually expressed as $S(\Theta)$, the shape factor (29). It can be shown that equation 7 holds once again.

$$r^* = \frac{2\gamma}{\Delta G_v} \qquad Eq.7$$

and

$$\Delta G^* = \frac{16\pi\gamma^3}{3(\Delta G_v)^2} S(\Theta) \qquad Eq.9$$

Thus homogeneous and heterogeneous nucleation can be related by equation 10.

$$\Delta G^*_{hetero} = S(\Theta)\Delta G^*_{homo} \qquad Eq.10$$

$S(\Theta) <= 1$ so one can see that $\Delta G^*_{hetero} < \Delta G^*_{homo}$ and heterogeneous nucleation will proceed with a smaller supersaturation concentration. Because of the presence of H_2O-insoluble particles in the atmosphere, heterogeneous nucleation is a common form of metastable droplet destabilization leading to efflorescence.

Experimental

Instrumentation

Sampling and chemical analysis of ambient aerosol can be done with a number of different methods. The impaction of aerosol onto filters which are later analyzed is the most commonly employed sampling method. The impaction method cannot be used for sampling metastable droplets, however, because upon impaction crystallization of solute would occur with the introduction of an artificial surface.

In-situ measurements, necessary in this case, can be made with nephelometry. Controlling the temperature and RH of the sample before it enters the nephelometer, allows the determination of the hygroscopic properties of the aerosol and partial determination of the composition. The impact of various temperatures and relative humidities on the air sample is determined by thermidography and humidography respectively. The impact of both is studied in these experiments with an integrated humidograph-thermograph system. The components of this system will be briefly described. Greater detail of the instrumentation has been presented previously (30,31).

The thermidograph measures the light scattering coefficient (b_{sp}) of an aerosol sample as a function of increasing temperature. Air entering the thermidograph passes through a preheater which vaporizes

all of the volatile components of the aerosol. It is then quickly cooled to room temperature. Components vaporized in the preheater will either recondense to small particles which can not scatter light well, diffuse to the walls of the cooler or both. The cooled aerosol enters a humidifier made of two concentric wetted walls. The outer wall is heated to a controlled temperature. The inner wall is not heated. The dew point temperature of the aerosol in the humidifier is determined by the heat flux through the outer heated wall. As the aerosol passes through the humidifier, it is exposed to an RH greater than 80%. The aerosol enters another heater, the internal temperature of which is scanned from ambient to $350^{o}C$, the entire scan of temperatures occurring within 3.5 min. Finally it is rapidly cooled again and enters an integrating nephelometer at a constant temperature and a RH value between 65 and 68%. The nephelometer measures the b_{sp} of the entering aerosol stream. Heater temperature data is stored in a microcomputer. The b_{sp} values are normalized to their maximum values and stored in the computer. Plots, known as thermidograms, are then generated of b_{sp} versus the heater temperature at which the b_{sp} was measured (Fig. 5). The graphs contain a great deal of information including the aerosols' deliquescent and hygroscopic properties as well as their thermal decomposition. Thermal decomposition of the H_2O and solute mass from the particles changes the amount of light scattered by the aerosol. From this decomposition curve, the initial composition of the aerosol can be inferred. Enough is known about the composition of aerosols and the light scattering ability of those components to be able to analyze these graphs with some detail. Such analysis has been done on laboratory generated aerosol as well as some ambient aerosol samples (30,31,32).

The humidograph measures b_{sp} of the air stream as a function of RH. Air entering the humidograph enters a wetted-wall humidifier and then is heated to $60^{o}C$ in 0.1 sec to decrease the RH of the aerosol to less than 20%. This RH decrease effloresces any aerosols with crystallization humidities less than 20% RH which may have deliquesced previously. The aerosol is then carefully cooled to increase the sample's RH to it's final value before entering the nephelometer. Conditions are maintained such that the highest RH the aerosol experiences is directly at the nephelometer inlet. The RH range is scanned by heating the wetted-wall humidifier continuously. Data of RH and b_{sp} are stored in the microcomputer. b_{sp} is normalized to its lowest RH value and a plot of normalized b_{sp} versus the RH value at the nephelometer inlet, a humidogram, is created. The humidogram (Fig 6) (31) shows the response of the aerosol to increasing RH, and so will include information on both the amount of dissolution of the aerosol before deliquescence and the deliquescence humidity of the aerosol.

The response of aerosol to decreasing RH can also be examined simply by exchanging the humidifier of the humidograph for the humidifier used in the thermidograph. As explained in the previous section, the aerosol is exposed to a RH greater to 80% in the humidifier and then is only exposed to

RHs lower than [illegible] aerosolized in the nebulizer. In this way, the particles are all exposed to an RH higher than their [illegible] and then exposed to gradually decreasing RHs. The combination of these two [illegible] studies of the entire hysteresis loop(33).

As mentioned previously, because of the compatibility of the humidograph and thermidograph, the two instruments are coupled into one system (Figure 7) (31).

Figures 5 & 6

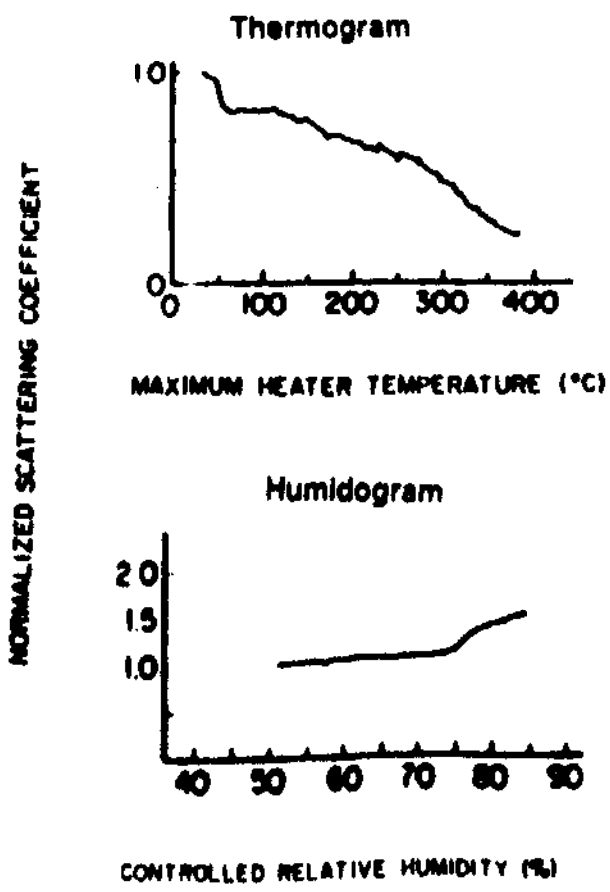

Figure 7

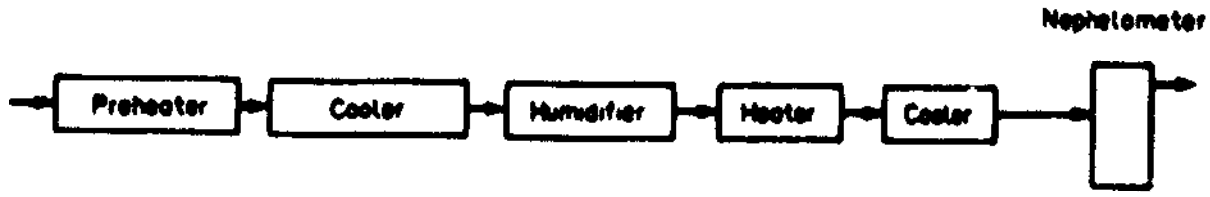

Thermidograph

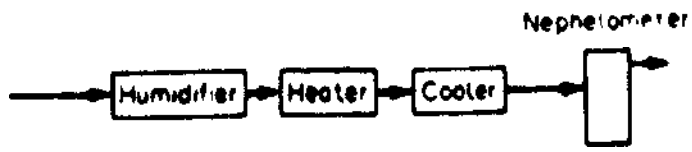

Humidograph

Integrated Thermidograph-Humidograph System

For field measurements at Grand Canyon, AZ, Mojave Desert, CA, and some of the measurements made in Riverside, CA, a somewhat different instrument, the thermograph, was employed. To bring the aerosol to the thermograph, air is drawn in through a stack 6 meters in height. It is passed through a cyclone which removes aerosols with diameters greater than 2 μm. The air stream is then split and one portion enters a reference nephelometer. The light scattering of the ambient, untreated air is measured. The other air stream enters the thermograph system. The incoming air is heated for 0.1 sec to a temperature which is increased from ambient to 350^oC during each test, then cooled to ambient temperature within 0.1 sec. It then enters an integrating nephelometer where its b_{sp} is measured at ambient temperature and relative humidity. A thermogram is then created by the microcomputer. The thermogram is a plot of b_{sp} normalized to its initial value at ambient conditions and corrected by the reference nephelometer values, versus the heater temperature.

Of particular interest is the thermogram region between 20^oC and 60^oC where the humidity the aerosol is exposed to is low enough that the liquid H_2O associated with the droplets is driven off. As the droplets are dried and rehumidified in the thermograph or thermidograph-humidograph, the hysteretic character of the droplets becomes important. In this temperature range liquid H_2O will be driven off the particle and then allowed to form around it again. Thus a droplet anywhere along the hysteresis curve (Fig.1) will be crystallized and then exposed to increasing humidity again (Fig. 1B, Curve a). Since metastable equilibrium can only be reached with decreasing humidities, metastable droplets will not reform under these conditions. b_{sp} of the aerosol will be decreased by the efflorescence of the metastable droplets. The presence of a steep decrease in b_{sp} signifies that the aerosol contained metastable droplets upon entering the instrument. A decrease in b_{sp} of at least 2% within this temperature range was taken to signify the presence of metastable droplets, due to the clarity of a 2% decrease in signal compared to noise present.

Thermidograph-humidograph sampling was done in Riverside, CA in the summer of 1983. Thermograph sampling was done in Riverside, CA, Mojave Desert, CA, and Grand Canyon, AZ. Riverside is an urban site influenced by maritime and continental air masses. Mojave Desert and Grand Canyon are rural sites dominated by continental air masses. The selection of these sites is of importance to the results in that the occurrence of metastable droplets, as viewed with the thermograms, can be compared between urban and rural aerosols, although not inseparable from the influence of the maritime air mass.

Sampling was done between July and September of 1984. During winter months, lower average RHs will be experienced causing a reduction in the percentage of metastable droplets seen. Also, with cooler ambient conditions, droplets are apt to freeze, causing another source of nucleation. Thus

metastable droplets are expected to be seen less often in winter than in the summer months of sampling.

Results

Filter samples were taken in Riverside, CA, simultaneously with humidograph measurement. Ambient deliquescence humidities for the droplets can then be compared to values predicted by the phase diagrams for given mixtures (21,22). This comparison assumes that $(NH_4)_2SO_4$ and NH_4NO_3 are the dominant compounds determining the deliquescent properties of the droplets, an assumption based on the dominance of the two compounds in sub-μm diameter aerosols. Figure 8 compares deliquescence of ambient droplets with values from the $NH_4NO_3/(NH_4)_2SO_4/H_2O$ phase diagram (Fig. 3). As previously discussed, the eutectic points give the first deliquescence humidity of the droplet (i.e. pts. a,b,c Fig.3), and the H_2O activity at the boundary between pure liquid and the solid/liquid region is the second deliquescence humidity for a given ratio of the two salts (curve d-e, Fig. 3). Ambient deliquescence was found to occur very close to the relative humidities predicted by the phase diagrams, but at slightly higher RH. This is due to the presence of components in the droplet other than pure $(NH_4)_2SO_4$ and NH_4NO_3. Other soluble compounds will decrease the water activity of the solution at any given concentration, raising the amount of H_2O necessary before deliquescence will occur. The deliquescence humidities of the $Na_2SO_4/(NH_4)_2SO_4/H_2O$ system were also compared to those found experimentally (Fig. 9). The agreement between the experimental and theoretical humidity values was almost unity. Thus, despite the complexity of the composition of an ambient droplet, trinary modeling is a valid approach to understanding a droplet's deliquescence.

We have discovered that metastable droplets occur in the ambient atmosphere with some frequency and that their impact on atmospheric chemistry and physics is not merely theoretical. Metastable droplets were seen at all three sampling sites with varying frequencies (Table 2). They were seen to exist more than 50% of the time when ambient RH was between 45 and 75% (Fig 10). Theoretical values predict that they would not be found at relative humidities greater than their deliquescent humidities, or less than their efflorescence humidities. Thus at RH < 30% and RH > 80%, very few metastable droplets should be seen. RH > 80% did not occur during any of the tests. RH < 30% did occur, however, with no occurrence of metastable droplets. Metastable droplets occurred with high frequency at 45%<RH<75%. For our sampling periods, RH values were found to be in this range an average of 38% of the time for the three testing sites (Fig. 11).

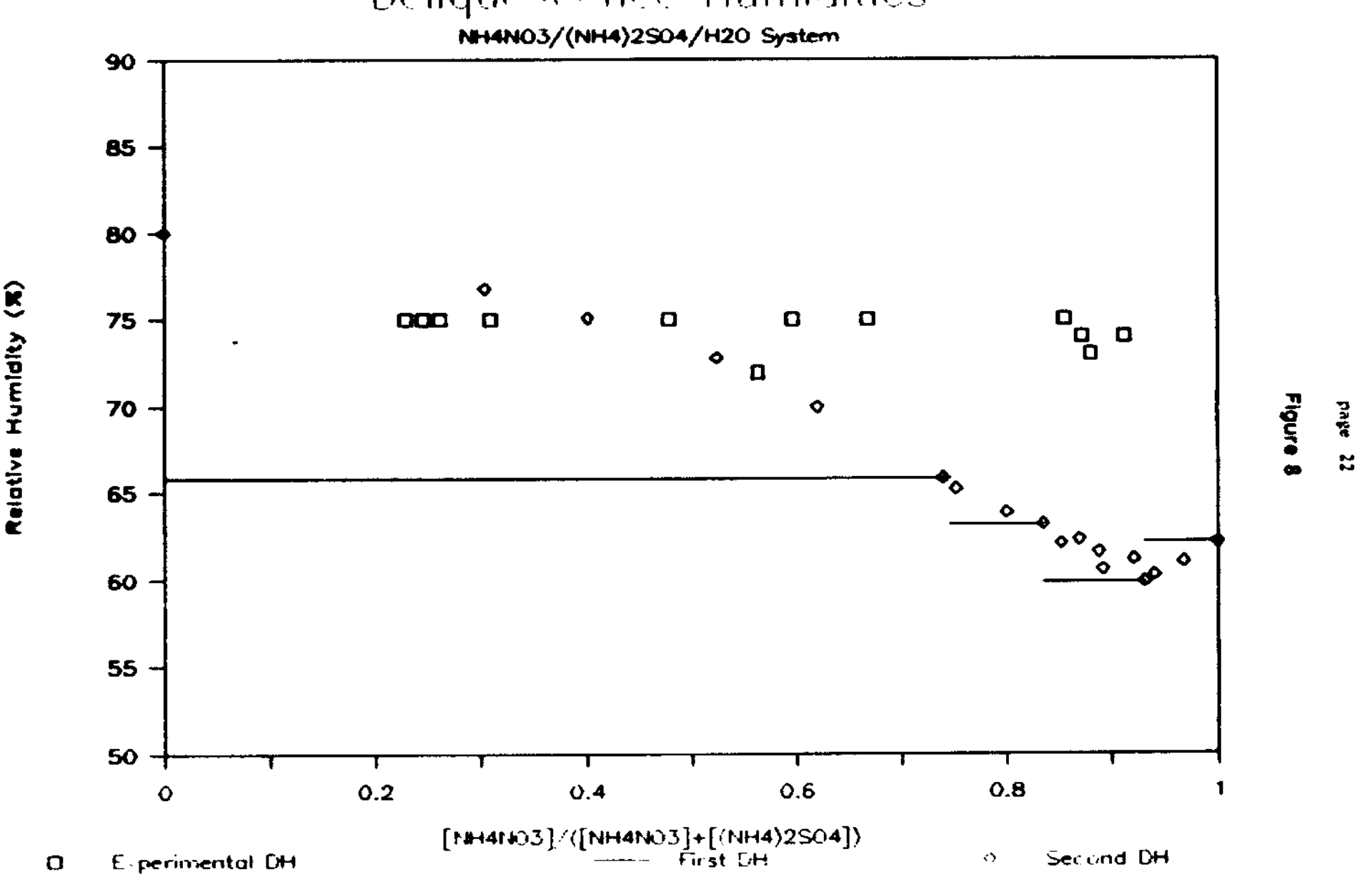
Deliquescence Humidities
NH4NO3/(NH4)2SO4/H2O System
Relative Humidity (%)
90
85
80
75
70
65
60
55
50
0
0.2
0.4
0.6
0.8
1
[NH4NO3]/([NH4NO3]+[(NH4)2SO4])
Experimental DH
First DH
Second DH

Figure 8

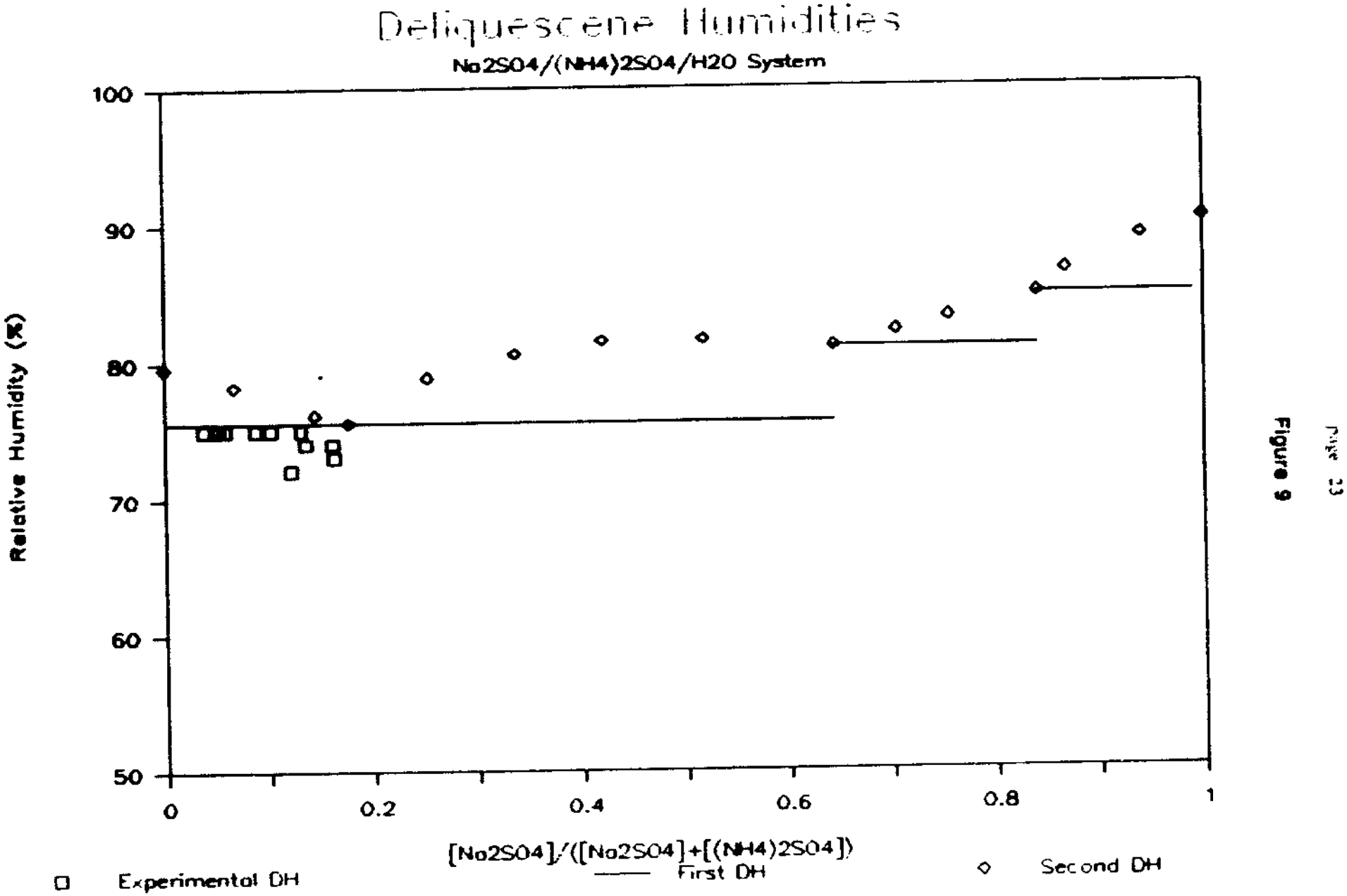
Deliquescene Humidities
No2SO4/(NH4)2SO4/H2O System
100
90
80
70
60
50
0
0.2
0.4
0.6
0.8
1
Relative Humidity (%)
[No2SO4]/([No2SO4]+[(NH4)2SO4])
Experimental DH
First DH
Second DH

Figure 9

Table 2

Summary of Sampling Results and Conditions

	Sampling Location		
	Grand Canyon	*Mojave Desert*	*Riverside*
Total # of Thermidograms	205	266	217
% of Thermidograms Used in Data Analysis	85%	96%	96%
% of Thermidograms Indicating Metastable Droplets	38%	10%	57%
Mean b_{sp} of Ambient Air $[10^{-5}m^{-1}]$ *(Particles with $d < 2\mu m$)*	1.05	2.61	25.1
Dates of Sampling	7/31/84 – 8/22/84	8/29/84 – 9/21/84	9/13/84 – 9/18/84

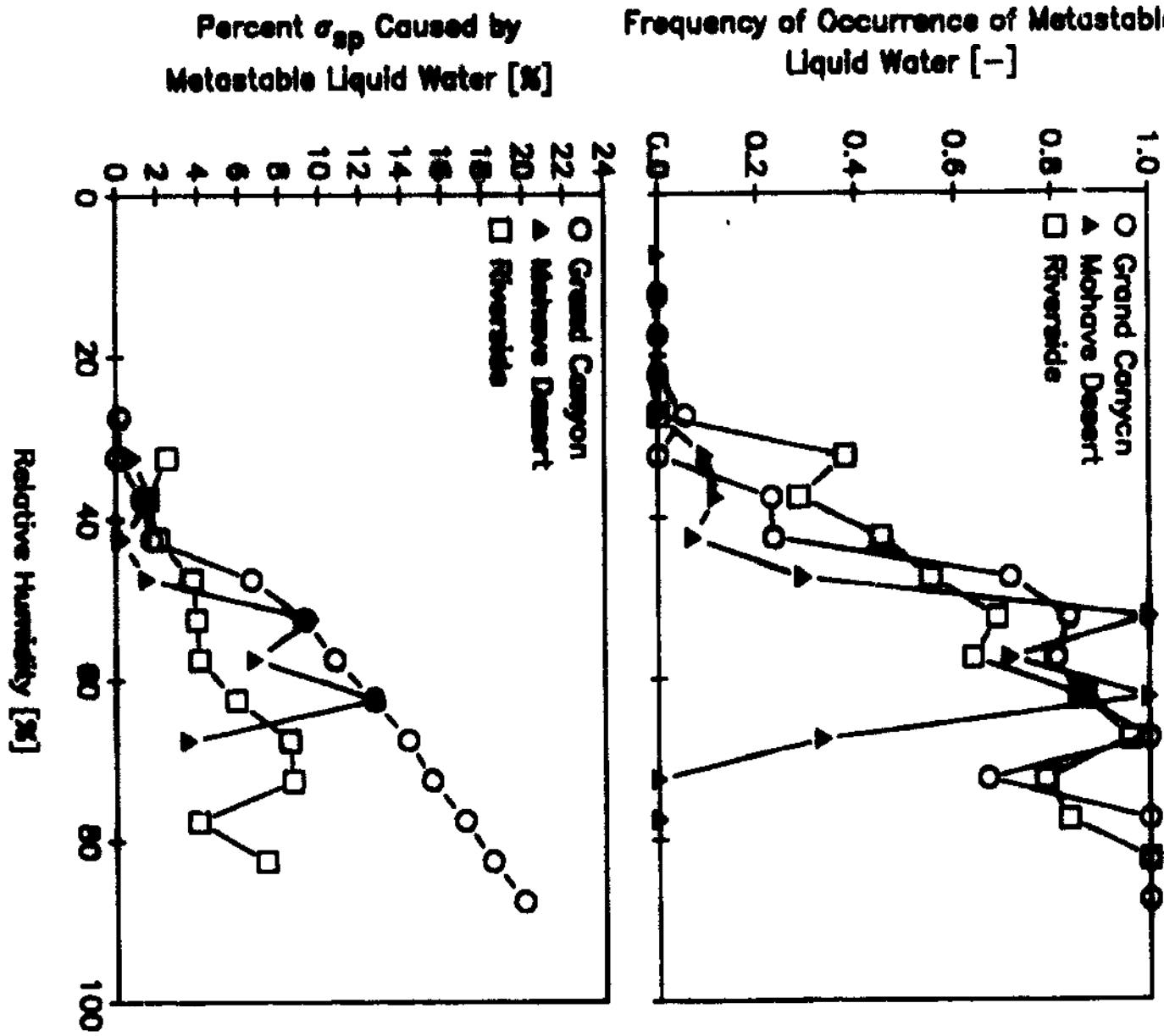

Figures 10 & 11

The amount of b_{sp} caused by metastable droplets was found to be appreciable whenever metastable droplets occurred with any frequency. The b_{sp} caused by by metastable liquid H_2O (Fig. 12) increased with RH between 30% and 80% RH. Within the range 45%<RH<75%, at least 5% of the light scattered by an aerosol sample was attributable to metastable droplets. At Grand Canyon, AZ, over 10% of the total light scattered was by metastable liquid H_2O when the RH was >55%. Over 10% of the total light scattering seen at Mojave Desert, CA also could be attributed to metastable droplets in certain ranges between 50–65% RH. This source of light scattering has not been taken into account when modeling ambient light scattering. The significant impact of metastable liquid H_2O on the scattering of light should be considered in future models.

The mechanism for the formation ambient metastable aerosol particles has yet to be determined. One explanation is that diurnal variations in RH create conditions favorable for their appearance. The southwestern U.S. experiences peaks in RH during late night/early morning hours. During the day the RH decreases. Aerosols would then also exhibit diurnal variations in the metastable state (11). Such a result was not seen, indeed, metastable droplets were found throughout the sampling period regardless of time of day. However, such a mechanism should not be discounted.

Aerosols exposed to different vertical regions of the atmosphere also may be exposed to conditions which result in metastable equilibria. Any given aerosol may travel hundreds of miles before being removed from the atmosphere. The amount of H_2O contained in vertical levels in the atmosphere varies according to elevation and meteorology. An aerosol exposed to varying RH during its travel may reach the metastable state.

Finally, an aerosol may be exposed to a constant RH, with a solute composition which changes during a chemical reaction to increase the particle's deliquescence humidity above that of the ambient RH. Any combination of these mechanisms could also result in metastable droplets.

Conclusion

Metastable droplets have been found to be common in the atmosphere. A significant portion of the ambient liquid H_2O content is attributable to metastable liquid H_2O in the RH range between 30% and 80%. These droplets contribute to light scattering to a large extent, but their influence on atmospheric physics and thermodynamics is as of yet undetermined. Considering the ubiquitousness of their existence, such questions deem further investigation in the future.

Figure 12

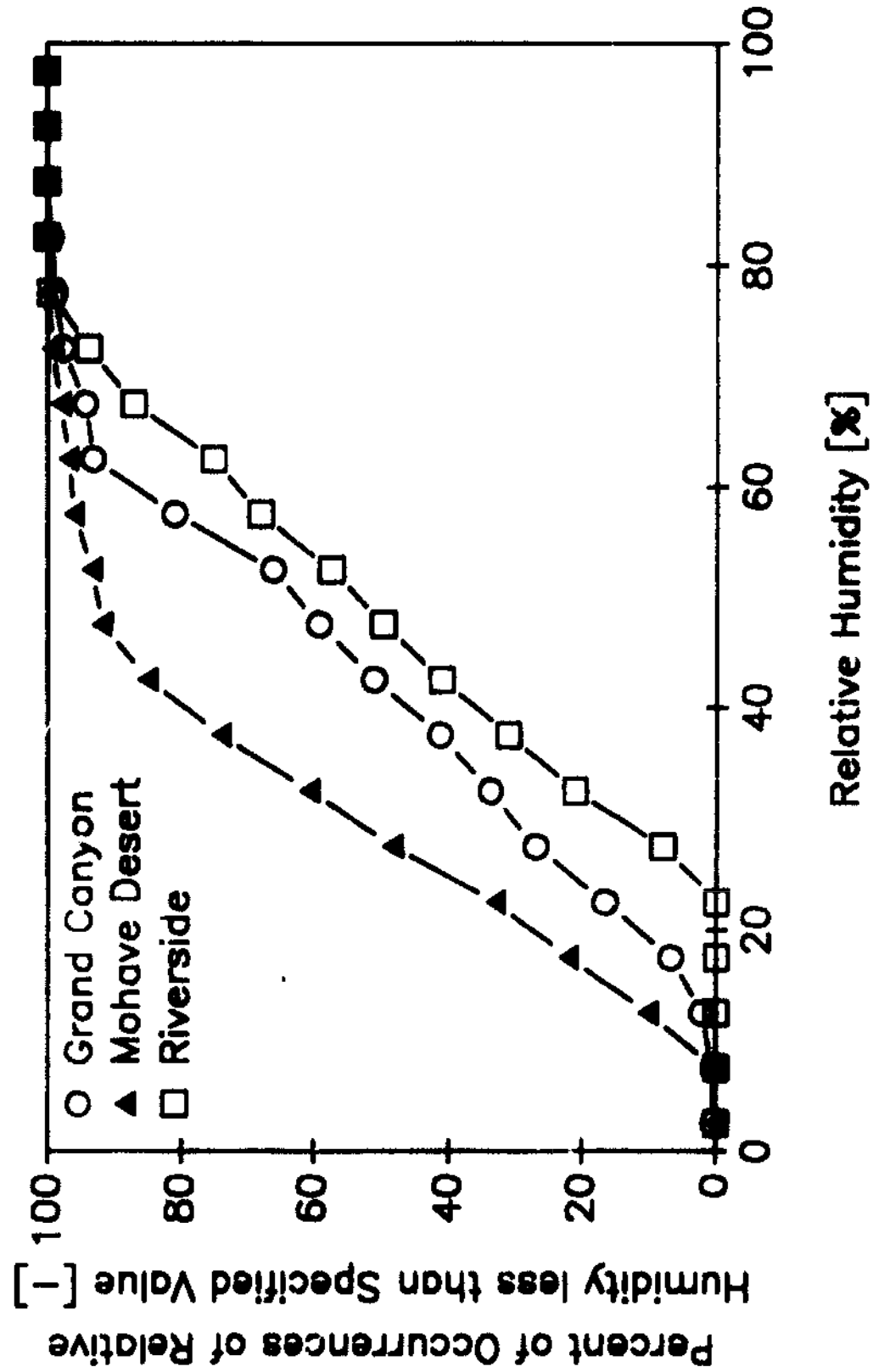
Percent of Occurrences of Relative Humidity less than Specified Value [–]
Relative Humidity [%]
0
20
40
60
80
100
Grand Canyon
Mohave Desert
Riverside

References:

1) Brosset, C. Atmospheric Environment, 12, 25-38 (1978).

2) Ono, A. Atmospheric Environment, 12, 753-757 (1978).

3) Dessens, H. Quart. J. Royal Meteor. Soc., 75, 23-26 (1949).

4) Freiburg, J. Environmental Sci. & Tech., 8, 8, 731-734 (1974).

5) Clarke, A.G., Williams, P.T. & Radojevic, M. 203-211, (1976).

6) Stelson, A.W. & Seinfeld, J.H. Atmospheric Environment, 16, 983-992 (1982).

7) Stelson, A.W. & Seinfeld, J.H. Atmospheric Environment, 16, 993-1000 (1982).

8) Meszaros, A. J. Aerosol Sci., 8, 31-38 (1977).

9) Fitzgerald, J.W. Atmospheric Environment, 14, 71-77 (1980).

10) Tang, I.N. Atmospheric Environment, 14, 819-828 (1980).

11) Rood, M.J., Covert, D.S., & Larson, T.V. Tellus, 39B, 383-397 (1987).

12) Pilinis, C. & Seinfeld, J.H. Atmospheric Environment, 21, 2453-2466 (1987).

13) Richardson, C.B. & Spann, J F. J.Aerosol Sci., 15, 563-571 (1984).

14) Tang, I.N. & Munkelwitz, H.R. J.Colloid Interface Sci., 98, 430-438 (1983).

15) Spann, J.F. & Richardson, C.B. Atmospheric Environment, 19, 819-825 (1985).

16) Cohen, M.D., Flagan, R.C., & Seinfeld, J.H. J.Phys.Chem., 91, 4563-4590 (1987).

17) Tang, I.N., Munkelwitz, H.R. & Davis, J.G. J. Aerosol Sci., 9, 505-511 (1978).

18) Stelson, A.W., & Seinfeld, J. H. Atmospheric Environment, 16, 2507-2514 (1982).

19) Spann, J.F., & Richardson, C.B. Atmospheric Environment, 19, 819-825 (1985).

20) Saxena, P. & Peterson, T.W., J.Coll.Interface Sci. , 79, 496-510, (1980).

21) Silcock, H.L. "Solubilities of Inorganic and Organic Compounds", V.3, Pt.2, Pergamon Press, 157-159 (1979).

22) Balej, J. & Thumova, M. Collection Czechoslov. Chem. Commun., 41, 3192-3203 (1976).

23) Ricci, J.E. "The Phase Rule and Heterogeneous Equilibrium", Dover Publications, New York (1966).

24) Seigneur, C., Pilinis, C. & Seinfeld, J.H. Atmospheric Environment, 21, 943-955 (1987).

25) Mirabel, & Katz, J. Chem. Phys., 60, 1138-1144 (1974).

26) Scott, W.D. & Cattell, F.C.R. Atmospheric Environment, 13, 307-317 (1979).

27) Murrell, J.N. & Boucher, E.A. "Properties of Liquids and Solutions", John Wiley & Sons (1982).

28) Zettlemoyer, A.C. "Nucleation", Marcel Dekker, Inc., New York (1969).

29) Porter, D.A. & Easterling, K.E. "Phase Transformations in Metals and Alloys", Van Nostrand Reinhold Company (1981).

30) Rood, M.J., Covert, D.C. & Larson, T.V. Aerosol Science Technol., 7, 57-65 (1987).

31) Rood, M.J., Larson, T.V., Covert, D.S., & Ahlquist, N.C. Atmospheric Environment, 19, 1181-1190 (1985).

32) Larson, T.V., Ahlquist, N.C., Weiss, R.E., Covert, D.C. & Waggoner, A.P. Atmospheric Environment, 16, 1587-1590 (1982).

33) Waggoner, A.P., Weiss, R.E. & Larson, T.V. Atmospheric Environment, 17, 1723-1731 (1983).

Author's Note

A summary of the conclusions and research presented here will appear in Nature in January 1989 in an article by Rood, M.J., Shaw, M.A., Larson, T.V., and Covert, D.S.

I would like to thank Dr. Mark Rood for overseeing and helping with this project as the project advisor, being a mentor throughout the last year, and helping with internship and graduate school searches simultaneously. Dr. Rood is a professor of Environmental Engineering.